



Protein from *red adzuki bean*: extraction optimization, glycosylation modification and physicochemical properties of glycation products

Meng Li¹ · Juliang Huang¹ · Yiming Chen¹ · Chang Liu¹ · Xiuli Wu¹

Received: 18 October 2023 / Accepted: 4 March 2024 / Published online: 22 April 2024
© The Author(s), under exclusive licence to Springer Science+Business Media, LLC, part of Springer Nature 2024

Abstract

In this study, the principle of alkali-solution and acid-isolation was used for the extraction of red adzuki bean protein (AP). The extraction conditions were optimized by response surface methodology to obtain the optimal extraction of AP with the highest yield of 87.1%. The solubility, water-holding capacity, oil-holding capacity, foaming and emulsification properties were explored. The results were as follows: The maximum solubility was 73.85% at pH 10.0. The water holding capacity decreased first and then increased with the increase in temperature, and the oil holding capacity tended to be the opposite. The foaming capacity and foaming stability increased with the increase of the concentration, while the emulsifying capacity tended to increase first and then decrease, and reached the maximum value of 71.71 m²/g when the protein concentration was 0.8% (w/v). Xylose, maltose and maltodextrin were used to modify AP by glycosylation reaction. The results showed that the glycosylation modification could effectively improve the solubility, foaming properties and emulsification properties of AP, which provided theoretical support for the future utilization of AP.

Keywords Response surface methodology · Red adzuki bean protein isolated · Glycosylation products · Physicochemical functional properties

Introduction

Red adzuki bean is also known as red bean, adzuki bean, leguminous cowpea [1], an annual herb. The protein content of red adzuki bean is about 20% [2], one-third of amino acids are essential amino acids [3], and the essential amino acid content has reached the FAO/WHO label. (Essential amino acid not less than 33.9%.) As a high-quality dietary protein, the digestion and absorption rate of red adzuki bean protein (AP) is high up to more than 50% [4].

In this study, the extraction method of alkali solubilization and acid precipitation was used. Alkali extraction and acid precipitation is the most commonly used method to

extract proteins from legumes, which is characterized by a balance of essential amino acids, high in vitro digestibility, emulsification, and water absorption [5]. Stone et al. [6] reported the extraction of pea proteins by alkali extraction and acid precipitation (1.0 M NaOH, pH 4.50) (yield 62.6%–76.7%) with good foaming stability (FS) and emulsification of the extracted proteins. Du et al. [7] investigated the effect of solid-fat ratio, pH, and temperature on the extraction rate of mung bean proteins at a The highest extraction rate of mung bean protein (77.32%) was achieved at a solid-fat ratio of 20 mL/g, pH of 9.10 and temperature of 40 °C. Boye et al. [8] used alkaline-complex ultrafiltration to extract proteins from peas, chickpeas and lentils. The results showed that the extracted proteins had good water retention, emulsification, foaming, and gelation properties.

Although AP has excellent functional properties, its quality was also reduced and its application was limited when environmental conditions changed. Modification is considered to be a promising way to enhance the functional properties of natural proteins. The purpose of protein modification is to modify certain molecular structures or chemical groups using appropriate methods, thereby improving target function without altering major functional and nutritional

✉ Chang Liu
liuc83@ccu.edu.cn

✉ Xiuli Wu
395113875@qq.com

Meng Li
220302132@mails.ccu.edu.cn

¹ College of Food Science and Engineering, Changchun University, No. 6543, Weixing Road, Changchun 130022, Jilin, China

properties [9]. Among these methods, glycosylation is one of the most promising methods to modify the functional properties of natural proteins, because it has the advantages of mild reaction process, stable modification products and no harmful products. Protein glycosylation, one of the most common but also one of the most complex post-translational modifications, is the covalent attachment of proteins to monosaccharides or polysaccharides, which not only contributes to the expansion of an organism's proteome beyond the genome's coding, but also has far-reaching impacts on protein function, stability, subcellular localization, and other traits.

At present, many researchers concentrated on the functional properties of AP, while investigations of protein modification and utilization were relatively scarce. In this study, the optimal conditions for protein extraction were obtained, and the glycosylation reaction was used to modify the protein, so as to further improve its functional properties. At the same time, we hope to provide theoretical basis for the modification of red adzuki bean protein.

Materials and methods

Materials

Red adzuki bean (produced in Jianping County, Liaoning Province, China); Bovine serum albumin was purchased from Shanghai Huishi Biochemical Reagent Co., LTD, Coomassil brilliant Blue G-250 was obtained from Qing dao Qing yao Biological Engineering Co., LTD, Bromocresol green, petroleum ether (Boiling range: 30–60 °C) methyl red, 95% were purchased from Aladdin Group: phthalaldehyde (OPA), β -mercaptoethanol were purchased from Merck, Potassium bromide, Potassium sulfate were obtained from Woke. ANS, xylose, maltose and maltose were purchased from Sinopharm Chemical Reagent (Shanghai, China).

Preparation of red adzuki bean protein

Red adzuki bean protein was obtained by alkali-solution and acid-isolation. In brief, red adzuki beans were ground into powder and sieved 100 mesh. Deionized water was added according to the solid–liquid ratio of 1:5 (w/v) and adjusted to a certain pH with 1 mol/L NaOH. After stirring at room temperature for 2 h, slurry was centrifuged at 3500 rad/min for 20 min. The precipitation was then extracted once according to the above solid–liquid ratio, and the two supernatants were combined. Then, adjust supernatant to pH 4.4 with 1 mol/L HCl. After centrifugation at 3500 rad/min for 20 min, 240 mL deionized water was added in precipitation and adjusted pH 7.0. Red adzuki bean protein (AP) was obtained by vacuum freeze-dried (FD-1A-50 vacuum

freeze-dryer Nanjing Xian Ou Instrument Manufacturing Co., LTD.) and was kept at -20 °C until further analysis.

Single-factor test experiment design

In this study, the effects of solid–liquid ratio (1:10–1:35), pH (8.5–11.0), temperature (30 °C–80 °C), and extraction time (30 min–80 min) were investigated on the extraction rate. Only one parameter was changed in each experiment while holding others.

Response surface experiment design

According to the results of the single-factor analysis, solid–liquid ratio, pH, temperature and time were selected as response factors, and the extraction rate was taken as response value. Design Expert 8.0 software was used to design the four-factor and three-level response surface experiment. The significance extraction rate of each variable was analyzed by software, and variance analysis. The variance analysis offers linear, quadratic, and composite interactions, through which their effects on the extraction rate were also studied by noting p values. The levels of experimental factors are shown in Table 1.

Preparation of protein–saccharide conjugates

By Pirestani et al. [10] description of the method with some modification. 0.8 wt% of protein sample and 0.8 wt% saccharides (xylose, maltose and maltose) were dissolved in a phosphate buffer solution (0.2 M, pH 7.0), stirred with a magnetic agitator at room temperature for 2 h to dissolve adequately. Then gently stirred overnight at 4 °C to fully hydrate the mixture. The pH of the solution was adjusted to 7.0 then heated at 90 °C for 10–50 min for conjugation, the reaction was terminated by immediately cooling in an ice bath.

After centrifuged at 4 °C (4000 rad/min, 30 min), the supernatant was lyophilized for protein–saccharide conjugates (AP-Xyl: protein-xylose conjugate, AP-Mal: protein-maltose conjugate, AP-MD: protein-maltodextrin conjugate) and kept at -20 °C until analysis. Protein, protein heated at 90 °C for 40 min (AP-H) and protein mixed with saccharides (M-AP-Xyl, M-AP-Mal and AP-MD represent for a mixture

Table 1 Design factors and level of response surface

Level	Solid–liquid ratio (w/v)	pH	Temperature (°C)	Time (min)
– 1	1:25	8.5	40	60
0	1:30	9	50	70
1	1:35	9.5	60	80

of protein with xylose, maltose and maltose, respectively) were used as controls.

Solubility

Solubility was measured by nitrogen dissolution index (NSI) using the method described by Li et al. [11] with some modifications. The pH values of sample solutions after dissolving in distilled water (5 mg/mL) were adjusted from 2 to 12 (pH 7 for protein–saccharide conjugates). After 30 min of stirring at room temperature, the samples were centrifuged at 3500 rad/min for 25 min. The protein content was determined by Coomassie bright blue G-250 method, and the total protein content was determined by Kjeldahl nitrogen determination method (Kjeldahl nitrogen determination Instrument Shanghai Fiber Instrument Co., LTD). The NSI was calculated according to Eq. (1):

$$\text{Nitrogen dissolution index/\% (NSI)} = \frac{\text{protein content in the supernatant}}{\text{total protein content in the sample}} \times 100\% \quad (1)$$

Water holding capacity

The water holding capacity was determined according to Wang et al. [12] with slight modification. One gram protein sample was added in 5 mL distilled water and stirred at room temperature for 30 min. After centrifugation at 3200 rad/min for 5 min, the precipitate was weighed, and the water holding capacity of red adzuki bean protein was calculated according to Eq. (2):

$$\text{Water holding capacity/\%} = \frac{\text{sample mass after centrifugation/g} - \text{sample dry mass/g}}{\text{sample dry mass/g}} \times 100\% \quad (2)$$

Oil holding capacity

The oil holding capacity was measured using a slight modification of the method of Lee et al. [13]. One gram protein sample was added in 5 mL corn oil (the saturated content of corn oil is high, the oil is not easy to oxidize, and the emulsion has good stability) and stirred at room temperature for 30 min, after centrifugation at 3200 rad/min for 5 min, the precipitate was weighed, and the oil holding capacity of red adzuki bean protein was calculated according to Eqs. (3):

$$\text{Oil retention/\%} = \frac{\text{sample mass after centrifugation/g} - \text{sample dry mass/g}}{\text{sample dry mass/g}} \times 100\% \quad (3)$$

Foaming capacity and foaming stability

The foaming capacity (FC) and FS were measured using the method of Liu et al. [14] with a slight modification. 10 mL sample solution (0.5–15.0 mg/mL) was homogenized for 1 min at 20,000 rad/min with a homogenizer (GF-1 high-speed shear machine Changzhou Runhua Electrical Appliance Co., LTD.). The total volume after foaming was measured several times within 0–60 min. Foam capacity (FC) was measured as the foam expansion rate at 0 min, and foam stability (FS) was measured as the foam expansion rate within 0–60 min. Foaming property is calculated according to formula (4):

$$\text{Foam expansion rate (\%)} = \frac{V - V_0}{V} \times 100\% \quad (4)$$

where V_0 and V are the volumes before and after homogenization, respectively.

Emulsifying properties

The emulsifying activity index (EAI) and the emulsion stability index (ESI) were measured by modifying the method of Liu et al. [14]. Dispersions containing 5 mL of corn oil and 5 mL of sample solutions (0.5 wt%–5 wt%) were homogenized at 20,000 rad/min for 1 min. At 0 min and 10 min pipetting 50 μ L from the bottom of the mixture was diluted to 5 mL with 1.0 mg/mL sodium phosphate buffer

(pH 7.0) containing SDS (0.1% w/v). The absorbance of the diluted emulsion was measured at 500 nm with sample zeroing. EAI and ESI are calculated according to formula (5) and (6):

$$\text{EAI (m}^2\text{/g)} = \frac{2 \times 2.303 \times A_0 \times N}{c \times \varphi \times \theta \times 10^4} \quad (5)$$

$$\text{ESI (min)} = \frac{A_0}{\Delta A} \times t \quad (6)$$

A_0 and A are the absorbance values measured at 0 and 10 min (500 nm) of the emulsion formation, respectively. $\Delta A = A_0 - A_{10}$; N is dilution ratio; C is protein concentration min; l is the path length of the test tube; I_o is the oil–water ratio.

Grafting degree (DG)

The DG of protein–saccharide conjugates was determined based on the loss of the free amino groups by OPA method according to Wang et al. [15]. The preparation of OPA reagent: 40 mg of OPA was dissolved in 1 mL methanol, with 20% SDS 2.5 mL, 0.1 mol/L of carbonate buffer solution 25 mL and 100 μ L of β -mercaptoethanol (2-ME), and the total volume was fixed to 50 mL. When the graft degree of the sample was measured, 4 mL of OPA reagent, 200 μ L of sample solution (protein concentration was 2 mg/mL) vortex dissolved and bathed at 35 °C for 3 min. The absorption was tested by UV–Visible spectrophotometer at 340 nm. Lysine was used as the standard substance to draw the standard curve, and DG of protein–saccharide conjugates was calculated according to Eq. (7):

$$\text{Grafting degree (DG/\%)} = (A_0 - A_1)/A_0 \times 100\% \quad (7)$$

A_1 represents the absorption of the sample. A_0 represents the blank absorption value obtained by replacing the sample with water. $A_0 - A_1$ is the net absorption value of the free amino group.

FTIR spectroscopy

Infrared spectroscopy and secondary structure analysis was carried out according the method of the method described by Wang and Sun et al. [16, 17] with some modifications. The freeze-dried samples were mixed with KBr powder (m/m, 1:100) and subjected to pressed to slice. The FTIR (Nicolet iS5, Thermo Fisher, USA) spectra were obtained over the range of 4000–400 cm^{-1} with a resolution of 4 cm^{-1} .

Color measurements

With colorimeter (Ci60, x-rite, USA) The color change of the sample is measured, and the E index is calculated according to Eq. (8):

$$\Delta E = (L^*2 + a^*2 + b^*2)^{1/2} \quad (8)$$

where L^* is the lightness index (0 = black, 100 = white); a^* (+ a^* = red, $-a^*$ = green) and b^* (+ b^* = yellow, $-b^*$ = blue); ΔE is the color characteristic [18].

Endogenous fluorescence

The sample was dissolved in a phosphate buffer solution (10 mM/L, pH 7.0) at a concentration of 10 mg/mL. The endogenous fluorescence was determined by fluorescence spectrophotometer (Hitachi F-2500 fluorescence spectrometer by Hitachi, Japan). The fluorescence intensity was tested at an excitation wavelength of 390 nm, excitation voltage was 400 V, slit width was 5 nm, and scanning speed was 300 nm/min. The emission spectra of samples at 300–500 nm wavelength were recorded [19].

Surface hydrophobic (Ho)

The surface hydrophobicity was determined by Hitachi F-2500 fluorescence spectrometer [20]. Four milliliters of 10 mg/mL protein sample was mixed with 20 μ L of ANS (80 mM/L). After vortex for 10 s, the samples were placed in the dark place for 3 min, and the blank control was the samples without ANS treatment. The emission wavelength was 400–600 nm, the emission and excitation slit was 5 nm, and the excitation wavelength was 390 nm. The surface hydrophobic (Ho) was expressed by the maximum fluorescence intensity.

Statistical analysis

All tests were performed in triplicate, and the data were expressed as the mean \pm standard error. SPSS 21.0 software was used to determine the significant differences. The mean values were compared using the one-way analysis of variance (ANOVA). $p < 0.05$ was defined as a significant difference between samples.

Results and discussion

The main components of adzuki bean and its protein

It can be seen from Table 2, the protein content in raw materials is relatively high, up to 17.12%, which is slightly lower than the study of Orsi et al. [21]. Meanwhile, the protein content of red adzuki protein powder was 78%, ash content 5.8%, fat 0.4% and moisture 7.68%.

Isoelectric point analysis of red adzuki bean protein

The absorbance reached its minimum value when the pH was 4.4 (Fig. 1), proving that the isoelectric point (pI) of the AP was approximately 4.4. When the pH reached the

Table 2 The main components of adzuki bean and its protein

Project	Protein%	Fat%	Moisture%	Ash content%
Adzuki bean	17.12 ± 0.46 ^b	0.85 ± 0.07 ^a	12.93 ± 0.88 ^a	3.08 ± 0.15 ^b
Adzuki bean protein	78.00 ± 0.53 ^a	0.40 ± 0.12 ^b	7.68 ± 0.67 ^b	5.80 ± 0.26 ^a

Results are showed as mean values ± SD in triplicate. Values in the same columns showing the different letter are different significantly ($p < 0.05$)

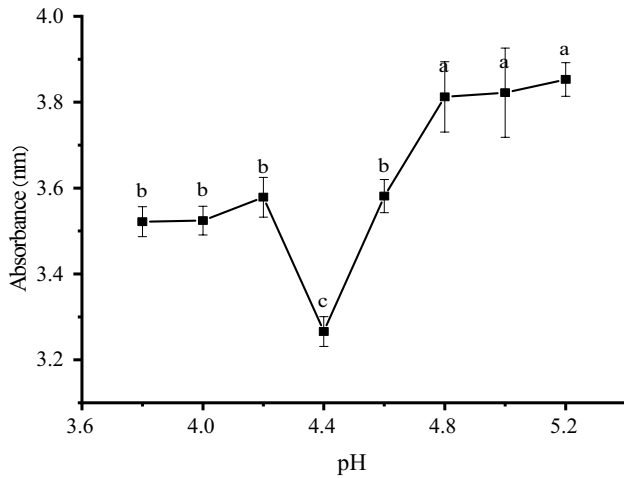


Fig. 1 Influence of different acid precipitation pH on absorbance. Different letters indicate significant differences at $p < 0.05$

isoelectric point, the positive and negative charges within the protein solution were equal and the net charge was zero. At this time, the electrostatic repulsion between proteins was minimized, which was conducive to the aggregation and precipitation of proteins.

Single-factor experiment analysis

Different solid–liquid ratios (1:10–1:35) were used during the extraction process for AP. As indicated in Fig. 2a, the extraction rate of AP gradually increased when the solid–liquid ratio was 1:10–1:30 (w/v). This was because the solute was fully dispersed as the solvent ratio increased, increasing the contact area between red adzuki bean powder and solvent, promoting the dissolution of protein. However, further increasing the solid–liquid ratio to 1:35 (w/v), which caused declines in the extraction rate due to the loss of

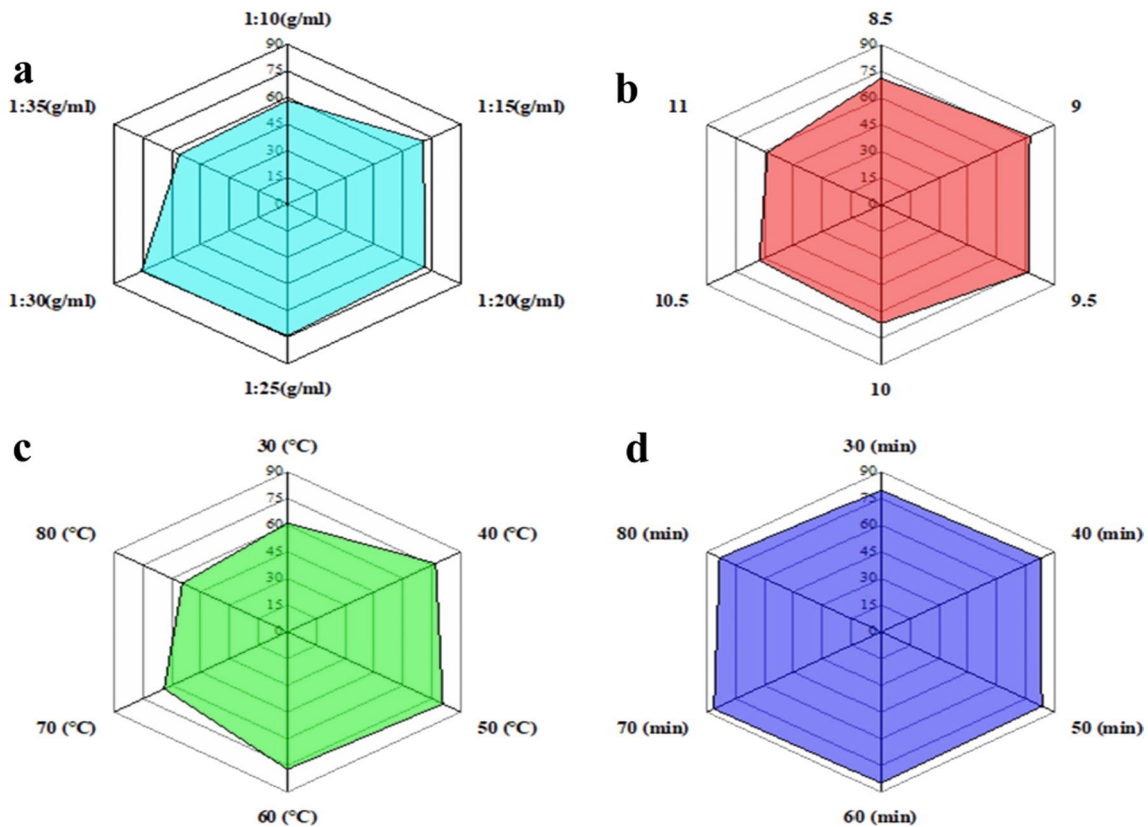


Fig. 2 Effects of different factors on the extraction rate of red adzuki bean protein **a** solid–liquid ratio, **b** pH, **c** temperature, **d** time

protein molecules caused by the presence of large amount of extraction solvent [22]. Hence, solid–liquid ratio of 1:30 (w/v) was selected for further optimization, and the maximum extraction rate of AP was 75.43% ($p < 0.05$).

The effects of the different pH (8.5–11.0) on the extraction ratio of red adzuki bean protein are presented in Fig. 2b. When pH is 9.0, the extraction rate of AP reaches the maximum of 77.21% ($p < 0.05$). It happened because the protein dissociates at pH 9.0 with a negative charge, and the repulsion between the charges increases its dispersion, promoting the dissolution of the protein. However, when the pH was greater than 9.0, the alkalinity was too strong to make protein denaturation, reducing the extraction rate of protein. These findings align with a previous study by He et al. [23]. As the pH increased above 11.0, the extraction rate of quinoa protein decreased, which could be attributed to the destruction of secondary bonds in the protein by strong bases, leading to denaturation of the protein's secondary and tertiary structure.

The effects of the different temperatures (30 °C–80 °C) on the extraction ratio of AP were presented in Fig. 2c. When the temperature reached 50 °C, the maximum extraction rate of AP reached 80.8% ($p < 0.05$), and the extraction rate began to decline as the temperature continued to rise. This is because an increase in temperature accelerates the speed of molecular motion, which makes the 3D structures of protein unstable. Consequently, this instability is conducive to the interaction between protein and water molecules, improving the solubility of AP. However, as the temperature continues to increase, the secondary bonds that maintained the advanced structure of the protein break, some hydrophobic groups inside the molecule are exposed to the molecular surface, and the protein molecules condense out through the hydrophobic interaction. This results in a decrease in the AP extraction rate.

The effects of the different times (30 min–80 min) on the extraction ratio of AP were presented in Fig. 2d, and reached the maximum 86.38% at 70 min ($p < 0.05$). Over time, the extraction rate of the AP begins to decline. This may be the result of flocculation and precipitation caused by the interaction between protein molecules precipitated during the long-term extraction.

Response surface analysis of red adzuki protein extraction

Results of response surface optimization experiment design

After selecting appropriate process parameters according to the results of the single factor test, Design Expert 8.0 was used to optimize the design. According to the design experiment of factors and levels in Table 1, the test results with

Table 3 Results of response surface optimization experiment design

Test number	Solid–liquid ratio (%)	pH	Temperature (°C)	Time (min)	Y Protein extraction rate (%)
1	1	−1	0	0	79.65
2	0	0	0	0	84.75
3	−1	0	0	1	84.15
4	1	0	−1	0	70.35
5	0	−1	0	0	84.6
6	0	−1	−1	0	69.75
7	0	0	1	−1	87.03
8	1	1	0	0	81.45
9	0	0	1	1	87.06
10	0	−1	1	0	79.35
11	0	0	−1	1	70.95
12	0	1	1	0	85.05
13	−1	−1	0	0	75.45
14	−1	1	0	0	81.15
15	0	0	0	0	84.45
16	0	1	0	1	82.05
17	0	−1	0	−1	79.05
18	1	0	0	−1	84.15
19	0	1	−1	0	70.35
20	1	0	1	0	87.45
21	0	−1	0	1	77.1
22	−1	0	1	0	86.85
23	−1	0	0	1	84.15
24	0	1	0	−1	82.65
25	0	0	0	0	85.05
26	0	0	−1	−1	75.3
27	0	0	0	0	85.95
28	−1	0	−1	0	70.03
29	1	0	0	1	83.25

protein extraction rate as response value were obtained, as shown in Table 3.

Variance analysis was conducted on the test result data obtained in Table 3. The quadratic multinomial regression fitting model of Y about Solid–liquid ratio, pH, temperature and time was obtained as follows: Withdrawal rate (%) $Y = 84.96 + 7.17 + 0.38 + 1.86 BC - 0.65 - D - 0.97 AB + 0.075 AC - 0.23 AD BC BD + 1.09 + 0.34 + 1.28 CD - 1.21 A^2 - 4.34 C^2 B^2 - 4.78 - 0.11 D^2$. Where: A represent the solid–liquid ratio (%); B represent the pH; C represent the temperature (°C); D represent the time (min). According to the analysis of variance and significance of the test results in Table 4, $p < 0.0001$ of the regression model indicates that the model is extremely significant. It is also known that the loss fitting term is $0.0602 > 0.05$, showing no significant results, indicating a good fitting effect. By observing F values of A, B, C and D, it can be

Table 4 Analysis of variance and significance of test results

Variable source	Sum of squares	Degree of freedom	Mean square	F value	<i>p</i> value
Model	921.01	14	65.79	45.07	<0.0001
Solid–liquid ratio (A)	1.69	1	1.69	1.16	0.3005
pH (B)	41.63	1	41.63	28.52	0.0001
Temperature (C)	616.91	1	616.91	422.61	<0.0001
Time (D)	5.03	1	5.03	3.45	0.0846
AB	3.80	1	3.80	2.60	0.1288
AC	0.023	1	0.023	0.015	0.9030
AD	0.20	1	0.20	0.14	0.7151
BC	6.50	1	6.50	4.45	0.0533
BD	0.46	1	0.46	0.31	0.5852
CD	4.80	1	4.80	3.29	0.0914
A ²	9.48	1	9.48	6.49	0.0232
B ²	122.18	1	122.18	83.70	<0.0001
C ²	148.13	1	148.13	101.47	<0.0001
D ²	0.078	1	0.078	0.054	0.8200
Residual error	20.44	14	1.48		
Misfit value	19.01	10	1.90	5.35	0.0602
Pure difference summation	1.42	4	0.36		
	941.45	28			

concluded that the main order affecting the extraction rate of AP is temperature > pH > time > solid–liquid ratio. R^2 is 0.9783 > 0.9, so the results of the model are consistent with the actual test results, which can be used to predict and optimize the extraction rate of AP.

Interaction analysis of each influencing factor

The response surface and contour map could reflect the interaction between various factors, the strength of the interaction between the two factors was directly proportional to the steepness of the response surface. The steeper the response surface was, the stronger the interaction between the two factors was. The shapes of the contour map were also an important factor in determining the strength of interaction. When the contour line was elliptical, the interaction between the two factors was strong, as shown in Fig. 3. The changing trend of the solid–liquid ratio and pH value curve surface is relatively steep. When the pH value is high, the extraction rate changes gently with the solid–liquid ratio. The extraction rate reaches the highest value when the solid–liquid ratio is 1:29–1:31 (w/v) (Fig. 3a). The change in solid–liquid ratio and the surface of the temperature curve was as steep as the pH (Fig. 3b). When the temperature was low, the extraction rate tended to be stable with the solid–liquid ratio. When the temperature was high, the extraction rate increased slightly first and then decreased. The curve surface variation trend of solid–liquid ratio and time was gentle (Fig. 3c), indicating that there was no significant effect between the two

conditions. The variation trend of pH and temperature curve surface was very steep (Fig. 3d). When the temperature was at a low level, extraction increased first and then decreased with the increase of solid–liquid ratio. The pH curve and the time curve surface have a gentle change trend (Fig. 3e). The extraction rate increased first and then decreased with the increase in pH. The curve surface of temperature and time is relatively flat (Fig. 3f), and the extraction rate gradually increased with the rise in temperature.

The optimal extraction conditions were obtained by software analysis: solid–liquid ratio 1:35 (w/v), pH 9.13, temperature 59 °C, time 79.37 min. At this time, the theoretical predicted value of AP extraction yield was 87.10%. According to the feasibility of the actual operation, the parameters were adjusted to the liquid–solid ratio of 1:35 (w/v), pH 9.0, temperature 59 °C, time 80 min, and three repeated verification tests. The extraction yield was 86.51%, which was basically consistent with the model. Therefore, the extraction parameters can be used to predict and analyze the real situation of the extraction rate of AP.

Functional property analysis of red adzuki bean protein

Solubility analysis

As can be seen from Fig. 4, the solubility curve presented regularly changes with the increase of pH. The solubility of AP was lowest when pH was near the isoelectric point

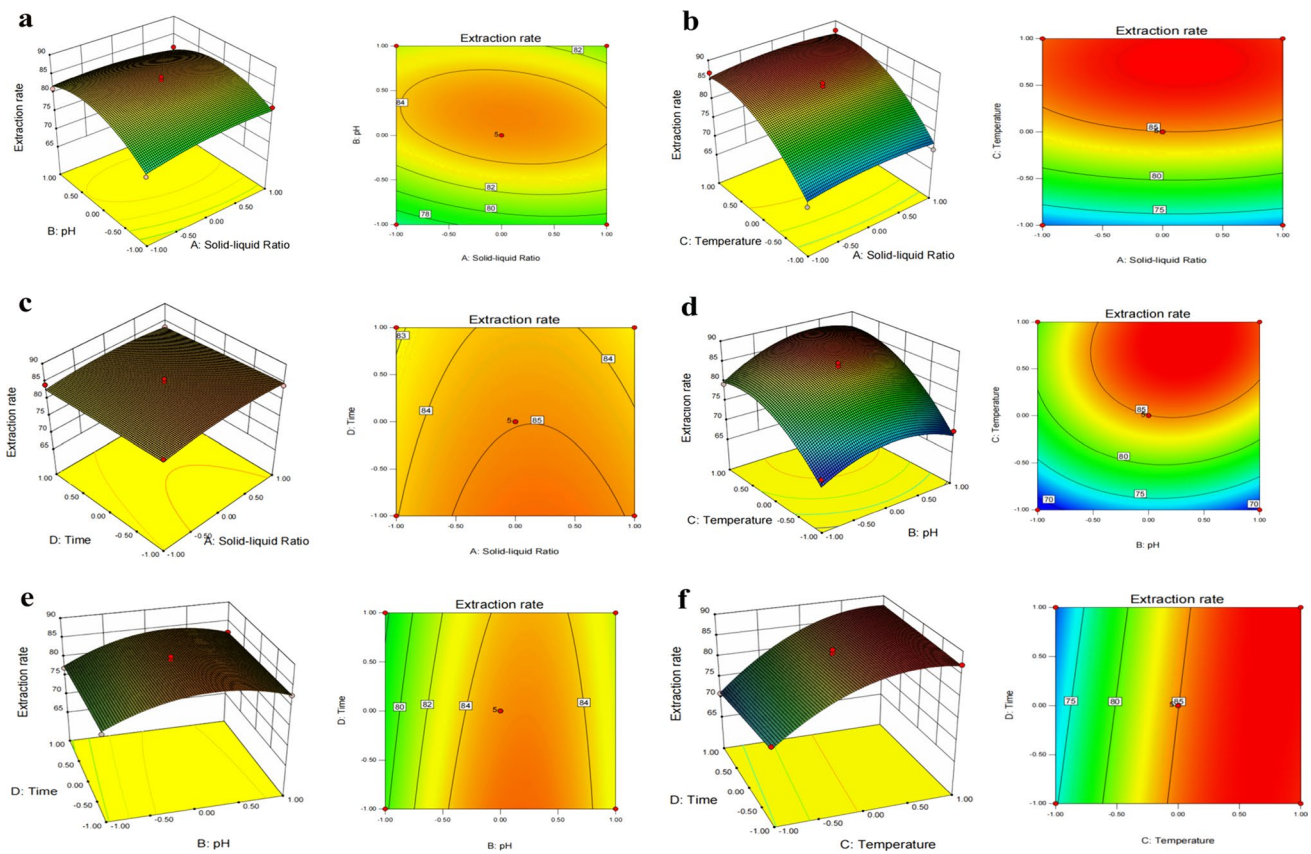


Fig. 3 **a** Effect of solid–liquid ratio and pH on AP extraction rate. **b** Effects of solid–liquid ratio and temperature on AP extraction rate. **c** Effects of solid–liquid ratio and time on AP extraction rate. **d** Effect

of pH and temperature on AP extraction rate. **e** Effect of pH and time on AP extraction rate. **f** Effect of temperature and time on AP extraction rate

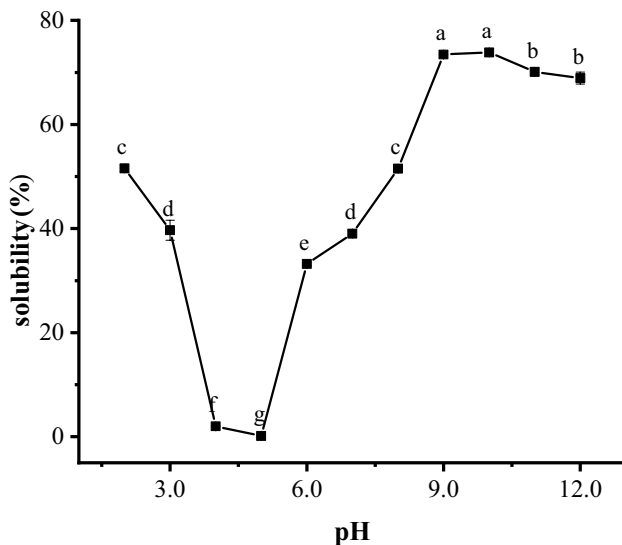


Fig. 4 Influence of different pH on solubility of adzuki bean protein. Different letters indicate significant differences at $p < 0.05$

of protein (approximately pH 5.0) owing to the net charge on the surface of protein molecules is close to zero, and the repulsive force between molecules is minimal, so protein is more likely to condense and form precipitation. When pH deviated from the isoelectric point, the surface of protein molecules has a net positive or negative charge, and its binding with water molecules is relatively stable, resulting in a gradual increase in solubility, which reached the maximum value of 73.85% ($p < 0.05$) at pH 10.0. However, pH is greater than 10.0, AP solubility gradually decreases, it may be caused by the denaturation of proteins due to excessive alkalinity [24], which was consistent with the conclusion reported by Yuliana et al. [25].

Water and oil absorption capacity

Water absorption capacity measures the ability of protein isolates to bind water. Water and oil absorption capacity are

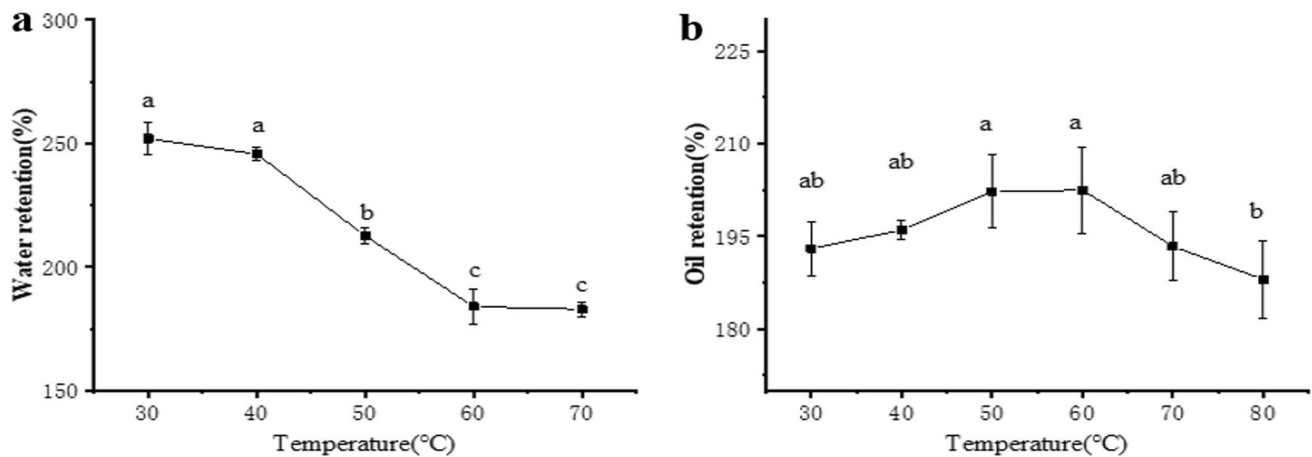


Fig. 5 **a** Effect of different temperature on water retention of adzuki bean protein. **b** Effect of different temperature on oil retention of adzuki protein. Different letters indicate significant differences at $p < 0.05$

important functional properties of the protein in the preparation of various food products [26].

As can be seen from Fig. 5a, with the gradual increase in temperature, the water holding capacity of AP gradually decreased and then became flat. Heat induction weakened the interaction by breaking the hydrogen bonds formed between the protein and water. Moreover, heating coagulates proteins, which reduced the surface area of proteins and decreased the effectiveness of binding polar amino acids to water [27]. Magyar et al. [28] also found that high temperatures could affect the internal structure of proteins.

The oil holding capacity of AP (a type of protein) was observed to increase slowly with temperature within the range of 30 °C to 50 °C. The oil holding capacity levelled off at temperatures between 50 and 60 °C and reached a maximum value of 202.44% at 60 °C (Fig. 5b). The significant decrease ($p < 0.05$) in the oil holding capacity of AP at the later stage may be attributed to the gradual stretching and dissociation of protein molecules with increasing temperature in the lower temperature range. After stretching, the peptide chains were more readily bound to small oil molecules, enhancing the oil holding capacity of AP. However, overheating caused the oil to become more fluid and thus weakened the protein–oil interaction, leading to a decrease in the oil holding capacity, which corresponds to the findings of Lee and Zhao et al. [13, 29].

Foaming capacity and foaming stability analysis

The foaming properties of proteins are very important in food processing [30]. FC refers to the ability of proteins to form foams under certain conditions (concentration, pH, and temperature); foam stability (FS) refers to the ability

of proteins to maintain foam volume over a certain time range. The influence of concentration on foaming property and foam stability of AP was shown in Fig. 6. As the concentration of protein increases, the foaming ability and foam stability of AP also tend to increase. This may be due to high protein concentration, which increased the viscosity of the protein solution, which contributed to the formation of the interfacial membrane protein. And with a larger AP concentration, the interaction between proteins favored the formation of a thicker adsorption film and enhanced foam stability [31]. Niu, Han and Wang found that quantity of protein Z was positively correlated with beer foam stability [32].

Emulsification and emulsification stability analysis

The emulsifying property of protein is significant in the application of food industry, such as beverages, cakes, desserts, mayonnaise, seasonings, milk, batter and coffee creamers [33]. Emulsifying properties can be described by emulsifying property (EAI) and emulsifying stability (ESI). The influence of concentration on EAI and ESI of AP is shown in Fig. 7.

As shown in Fig. 7a, the EAI of AP showed a trend of first significant increase ($p < 0.05$) and then decreased with the increase of concentration. When the AP concentration was 0.8%, the EAI reached the maximum (71.71 m^2/g). As shown in Fig. 7b, ESI of AP first decreased and then significantly increased ($p < 0.05$). When the AP concentration was 0.8%, ESI reached the minimum value of 11.8 min.

The dependence of EAI activity on protein concentration can be explained by kinetic absorption. When the protein concentration is high, the activation energy

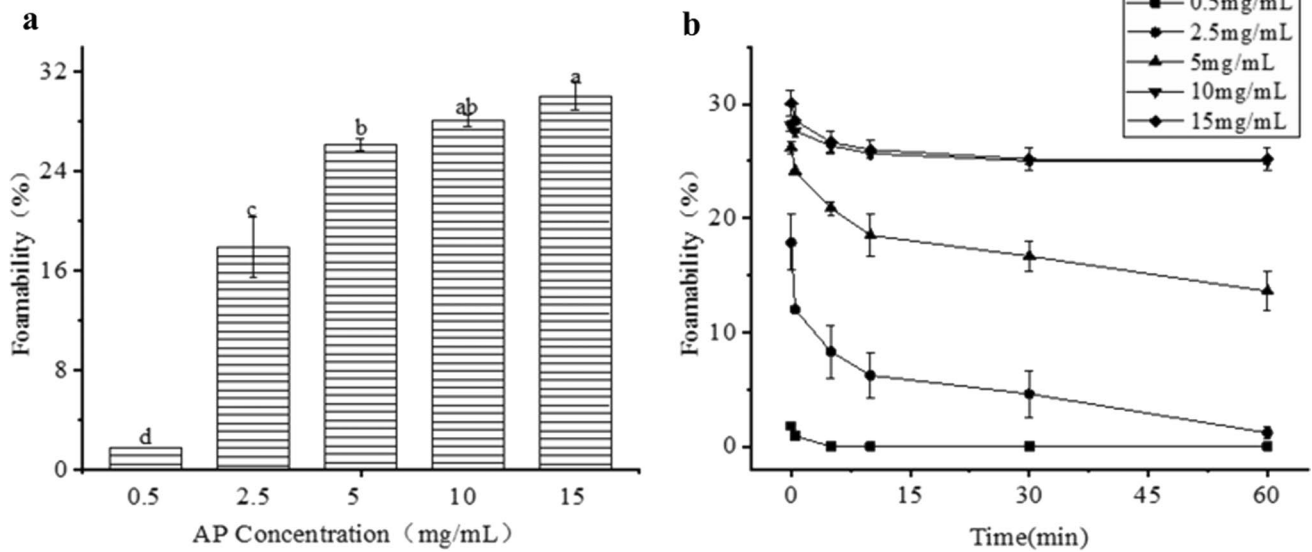


Fig. 6 a Effect of concentration on foamability of adzuki protein. b Influence of concentration on foamability of adzuki protein. Different letters indicate significant differences at $p < 0.05$

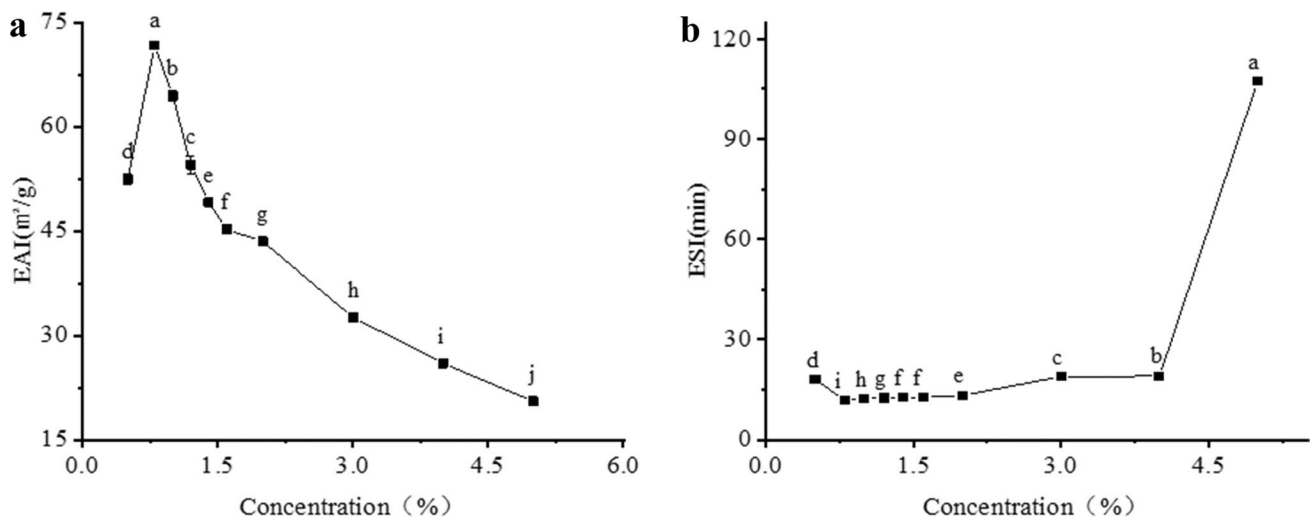


Fig. 7 a Effect of concentration on emulsification of adzuki protein. b Effect of concentration on emulsion stability of adzuki protein. Different letters indicate significant differences at $p < 0.05$

barrier restricts the diffusion and movement of the protein. When the protein concentration is low, protein molecules can participate in the emulsification process more quickly. Emulsification stability change tendency is due to the thickness of the interface film increasing with the increase of protein concentration, so the strength of the film and the ESI of AP are enhanced [34]. It agreed with a previous finding where an increasing concentration of soy protein isolates (SPI) had the same effect on the interfacial pressures and adsorption kinetics at the oil–water interface [35].

Analysis of functional properties of glycosylated modified products of red adzuki bean protein

Determination of grafting degree

The OPA method was used to measure the content of free amino groups in proteins to evaluate the degree of Maillard reaction. The principle was that during the glycosylation, the free amino group in proteins reacted with the carbonyl group of reducing sugar to reduce the amount of free amino groups in proteins [36]. Figure 8 shows the grafting degree of the

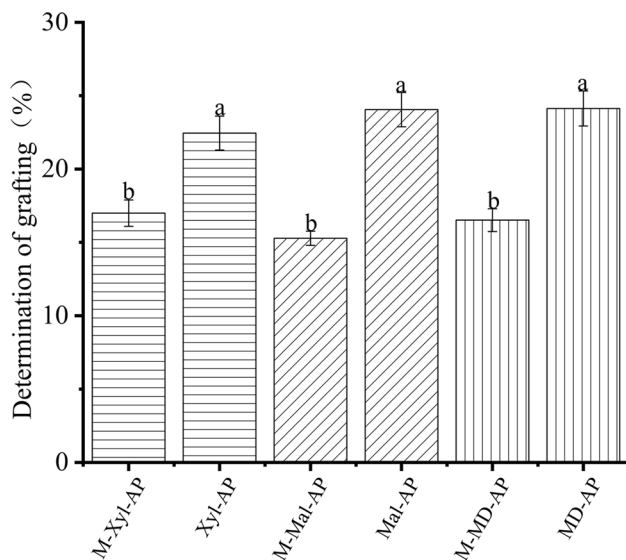


Fig. 8 Grafting degree of glycosylation products and mixtures of three sugars and proteins. Xyl-AP, xylose glycosylated protein; Mal-AP, maltose glycosylated protein; MD-AP: maltodextrin glycosylated protein; M-Xyl-AP: Xylose and protein mixture; M-Mal-AP: mixture of maltose and protein; M-MD-AP: maltodextrin and protein mixture

mixture of AP and different sugars at room temperature and Maillard reaction products obtained after mixing and heating at 90 °C for 40 min. After glycosylation, the content of free amino group decreased in different degrees, which led to a significant increase in the grafting degrees in different protein–saccharide conjugates ($p < 0.05$).

FTIR analysis

Glycosylation is the initial stage of the Maillard reaction. It is the dehydrated condensation of reducing sugars with proteins to form N-glucamine. N-glucamine undergoes irreversible Amadori electron rearrangement to form a protein conjugate to saccharides with a 1-amino-1-deoxyketose structure, a process that consumes the primary amino group of the amino acid. Fourier transform infrared spectroscopy (FTIR) was used to analyze the secondary structure of samples. The commonly used absorption bands for protein structure include the amide I band (1600–1700 cm^{-1}), which is mainly due to H–O–H bending vibration and C=O stretching vibration, the amide II band (1480–1575 cm^{-1}), which is mainly due to N–H bending vibration, the amide III band (1260–1330 cm^{-1}), which is mainly due to C–O–C and C–O vibration. Most of the characterization of glycosylated proteins is based on the amide II band [37].

Figure 9 shows the infrared spectra of samples. The characteristic structure of sugar chain was generally around $\sim 3300 \text{ cm}^{-1}$, which was mainly caused by hydroxyl stretching. The three glycosylated protein samples showed

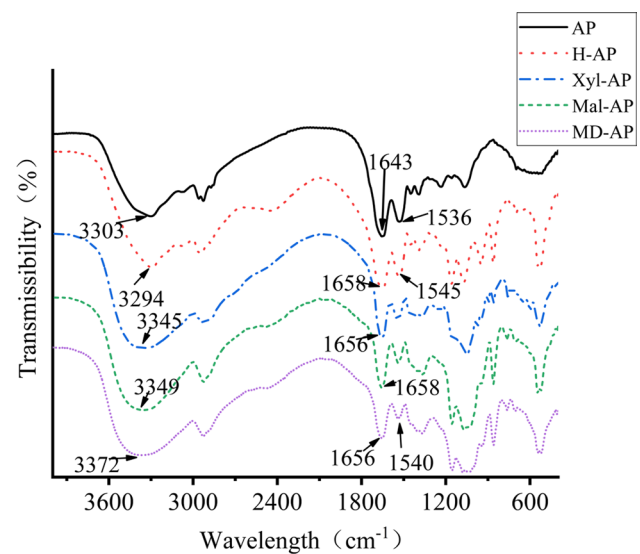


Fig. 9 Infrared spectra of adzuki bean protein and its glycosylated products. AP: red bean protein; H-AP: red bean protein heated at 90 °C for 40 min; Xyl-AP, xylose glycosylated protein; Mal-AP, maltose glycosylated protein; MD-AP: maltodextrin glycosylated

wider absorption peaks at $\sim 3300 \text{ cm}^{-1}$, which was attributed to an increase in the amount of –OH, this phenomenon indicated a reaction between all three saccharides and AP. The absorption band at 1536 cm^{-1} was reported to be mainly attributable to the primary amino group. After glycosylation, the absorption peak intensity of AP at 1536 cm^{-1} reduced due to the consumption of amino acid residues during the Maillard reaction. The amide I absorption band at 1643 cm^{-1} was caused by the spectral overlap of the C=O group, with in-plane –NH bending and C=N bond. The absorption peak of 1643 cm^{-1} in AP migrates to 1658 cm^{-1} and 1656 cm^{-1} , which proved the formation of Schiff bases containing C=N structure. It was shown that the primary amino group of AP reacted with the carbonyl group of reducing sugar after dehydration and condensation to produce Schiff base products [38].

The change of protein secondary structure can be reflected by the amide I band [39], absorption peaks of 1650 cm^{-1} – 1660 cm^{-1} corresponding to α -helix, 1610 cm^{-1} – 1640 cm^{-1} corresponding to β -folding, 1660 cm^{-1} – 1700 cm^{-1} corresponding to β -angle and 1640 cm^{-1} – 1650 cm^{-1} corresponding to random crimp stretching vibration were selected, OMNIC software was used for second-order derivation to calculate the changes of secondary structure content of glycosylated products (Table 5). AP had the highest content of α -helix and β -folding in all samples, and the lowest content of β -angle and random curling. This may be due to the introduction of sugar chains which can destroy hydrogen bonds in α -helix and β -folding structures, leading to the development of

Table 5 Secondary structure content of each sample

Sample	Alpha helix (%)	Beta folding (%)	Beta angle (%)	Random crimp (%)
AP	21.25 ± 0.01 ^a	34.12 ± 0.01 ^a	38.76 ± 0.00 ^e	5.87 ± 0.01 ^e
H-AP	19.58 ± 0.01 ^b	31.59 ± 0.00 ^b	40.06 ± 0.01 ^d	8.35 ± 0.00 ^c
Xyl-AP	–	29.09 ± 0.01 ^c	63.58 ± 0.00 ^a	7.33 ± 0.01 ^d
Mal-AP	14.02 ± 0.00 ^c	27.36 ± 0.02 ^d	41.58 ± 0.01 ^c	9.25 ± 0.02 ^a
MD-AP	10.13 ± 0.01 ^d	22.47 ± 0.01 ^e	45.03 ± 0.01 ^b	9.23 ± 0.01 ^b

Results are showed as mean values ± SD in triplicate. Values in the same columns showing the different letter are different significantly ($p < 0.05$)

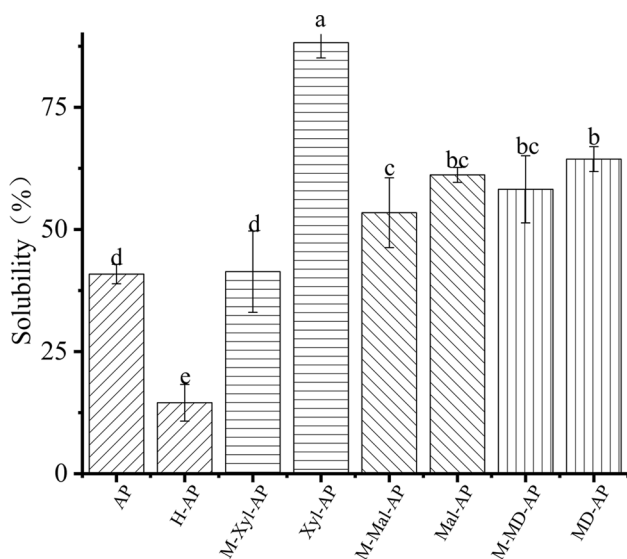


Fig. 10 Solubility of adzuki protein mixture with glycosylation products. AP: red adzuki bean protein; H-AP: protein heated at 90 °C for 40 min; Xyl-AP, xylose glycosylated protein; Mal-AP, maltose glycosylated protein; MD-AP: maltodextrin glycosylated protein; M-Xyl-AP: mixture of xylose and protein; M-Mal-AP: mixture of maltose and protein; M-MD-AP: mixture of maltodextrin and protein

protein peptide chains, exposure of internal groups, and changes in protein spatial conformation. Glycosylation caused a decrease in the α -helix content and an increase in the random coil content, which was probably attributed to the unfolding of protein structure and partial secondary structure transformation from α -helix into random coil during the glycosylation reaction [16]. The result was corresponding to the work of Sun et al. [17], they found a reduction in the β -sheet content of glycosylated hemoglobin reduces resistance to enzymatic digestion, making them favorable for enzymatic hydrolysis.

Solubility analysis

Figure 10 shows the solubility of the glycosylated products at pH 7.0. After heat treatment, the solubility of AP (40.86%) decreased significantly to 14.52% ($p < 0.05$), which may be caused by the formation of insoluble protein aggregates due

to the denaturation of proteins caused by heating [40]. The solubility of protein–saccharide conjugates in three groups was significantly higher than that in AP and unreacted mixed groups ($p < 0.05$). AP-Xyl showed the most outstanding solubility performance, which was 115.93% higher than AP.

The solubility of three groups of samples was higher than the AP and the mixture, which indicated glycation treatment produced compounds with higher water solubility, and xylose glycosylation product had the best effect. The reason for this was the smaller the molecular weight of the saccharide, the more carbonyl was reduced at the same mass, so it was easier to contact and react with the protein. In addition, higher molecular weight sugars may cause steric hindrance and limit the reaction [41]. Luo et al. [42] also came to the same conclusion.

Foaming capacity and foaming stability

Figure 11 shows the FC and FS of protein and protein–saccharide conjugates. The FC and FS of the protein–saccharide conjugates in the three groups were greater than those in the AP and unreacted mixed groups (foaming at 0 min: AP 33.33%; Xyl-AP 52.38%; Mal-AP 52.381%; MD-AP 53.12%, foaming at 60 min: AP 21.05%; Xyl-AP 47.37%; Mal-AP 48.28%; MD-AP 50.00%). The reason for this phenomenon may be that after glycosylation, hydrophilic saccharide chains covalently bind to protein molecules, and the introduction of a large number of hydroxyl groups increases the electrostatic attraction between protein molecules, thus enhancing the thickness and hardness of the foam layer and improving the foaming property and foam stability [43].

Emulsifying properties analysis

The emulsion is a system which can be divided into two immiscible phases: water phase and oil phase. Proteins can be adsorbed to the oil–water interface, carbohydrates have relatively high solubility in the aqueous medium, protein molecules with oil adsorption capacity and high hydrophilic saccharide molecules combine, so that their conjugated products form a strong solvation layer near the oil–water

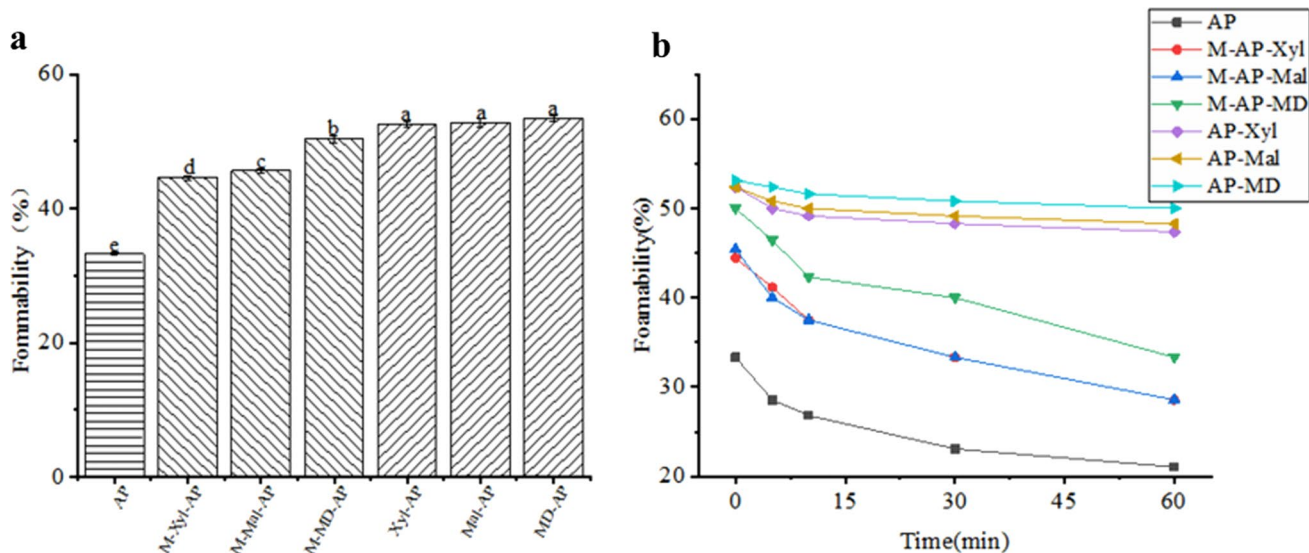


Fig. 11 **a** Foaming capacity of protein–saccharide mixture and glycosylation products. **b** FS of protein–saccharide mixture and glycosylation products. Different letters indicate significant differences at $p < 0.05$. AP: red adzuki bean protein; Xyl-AP, xylose glycosylated

protein; Mal-AP, maltose glycosylated protein; MD-AP: maltodextrin glycosylated protein; M-Xyl-AP: Xylose and protein mixture; M-Mal-AP: mixture of maltose and protein; M-MD-AP: maltodextrin and protein mixture

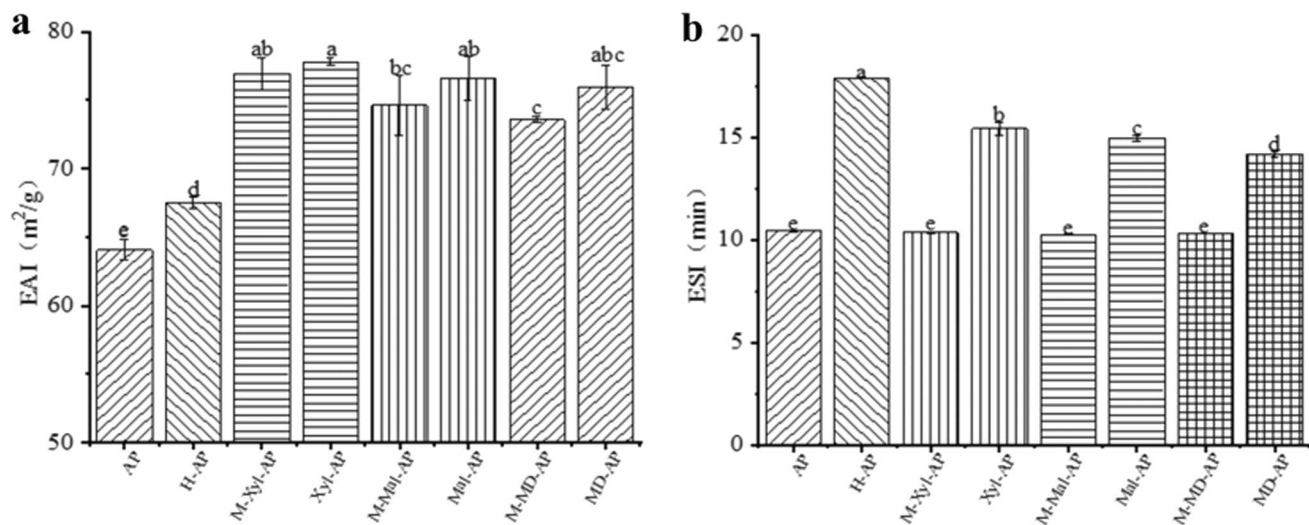


Fig. 12 **a** Emulsification of protein–saccharide mixture and glycosylation products. **b** Emulsification stability of protein–saccharide mixture and glycosylation products. Note: Different letters indicate significant differences at $p < 0.05$. AP: red adzuki bean protein; H-AP: protein heated at 90 °C for 40 min; Xyl-AP, xylose gly-

cosylated protein; Mal-AP, maltose glycosylated protein; MD-AP: maltodextrin glycosylated protein; M-Xyl-AP: mixture of xylose and protein; M-Mal-AP: mixture of maltose and protein; M-MD-AP: mixture of maltodextrin and protein

interface. Thus, the spatial stability of the oil droplets in the emulsion is enhanced [44]. First, the covalently crosslinking between protein and saccharide makes the protein structure unfolded and some hydrophobic groups contained in the interior structure of native protein expose to the molecular

surface to increase the lipophilicity of conjugates. Secondly, the saccharide chains with many hydrophilic groups endow conjugates an increased hydrophilicity [44].

Figure 12 showed the emulsification and emulsification stability of the mixture of AP and protein–saccharide

conjugates. Compared with AP (64.06 m²/g, 10.43 min), emulsification and emulsification stability were significantly improved after glycosylation ($p < 0.05$), and Xyl-AP had the best EAI (77.82 m²/g) and ESI (15.4 min).

The increased emulsification activity was probably explained by the exposure of hydrophobic groups in the proteins after glycosylation, which made some protein molecules more soluble in the oil phase, and the hydrophilic nature of the sugars, which also enhanced the emulsification activity. Bu et al. [45] found that higher solubility can promote the adsorption and dispersion of proteins in the emulsified phase, which is consistent with this work. Zhu et al. [46] found pea protein isolate (PPI) and xylo-oligosaccharide (XOS) glycosylated conjugates (PPI-MRPS) exhibited better solubility and emulsifying properties compared with physical mixture (PPI-XOS) and PPI.

Color measurements analysis

Table 6 showed the color properties of protein–saccharide conjugates. AP had the highest a^* value and b^* value, while the lowest L^* value, this may be because of the red color of seed coat. The closer the brightness value L^* is to 100, the more obvious the white color is. The value of a^* is positive, indicating red color, negative a^* represents green color. If b^* is positive, it means yellow color; if it is negative, it means blue color. The color difference ΔE represents the total color change [47].

When AP had been treated by heating, the a^* value and b^* value was reduced, owing to the destroy of glyxogroup on C3 of anthocyanin and byproducts produced [48]. When the AP is glycosylated, the increase in redness and yellowness may due to the Maillard reaction [49], as compared with the mixture of protein and saccharides. AP-Xyl had the highest a^* and b^* values among the three protein–saccharide conjugates., which may be associated with the highest degree of glycosylation of xylose with proteins.

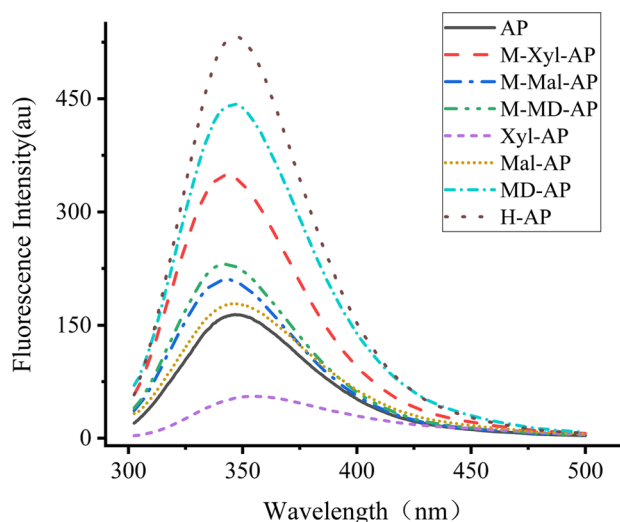


Fig. 13 Endogenous fluorescence spectra of adzuki protein mixture and glycosylation products. AP: red adzuki bean protein; H-AP: protein heated at 90 °C for 40 min; Xyl-AP, xylose glycosylated protein; Mal-AP, maltose glycosylated protein; MD-AP: maltodextrin glycosylated protein; M-Xyl-AP: mixture of xylose and protein; M-Mal-AP: mixture of maltose and protein; M-MD-AP: mixture of maltodextrin and protein

Endogenous fluorescence analysis

Figure 13 showed the endogenous fluorescence spectra of protein–saccharides conjugates. The endogenous fluorescent chromophore group exposed in AP such as tryptophan, tyrosine, and phenylalanine residues emit fluorescence. When the protein structure was stretched, the fluorescence intensity decreased [50]. The change of protein conformation can be indirectly determined by measuring the change of AP fluorescence intensity before and after modification. Compared with AP, the peak intensity of fluorescence emission peak of H-AP increased significantly, which was related

Table 6 Chromaticity of adzuki protein mixture and glycosylation products

Sample name	L^*	a^*	b^*	ΔE
AP	66.45 ± 0.23 ^f	11.60 ± 0.06 ^a	20.67 ± 0.18 ^a	70.55 ± 0.25 ^f
H-AP	101.97 ± 0.50 ^{ab}	3.84 ± 0.20 ^{cd}	13.23 ± 0.45 ^d	102.9 ± 0.44 ^{ab}
M-Xyl-AP	91.73 ± 4.34 ^d	7.09 ± 1.49 ^b	15.13 ± 1.15 ^c	93.26 ± 3.99 ^{de}
M-Mal-AP	96.13 ± 0.39 ^{cd}	4.78 ± 0.09 ^c	12.87 ± 0.22 ^{de}	97.11 ± 0.35 ^{cd}
M-MD-AP	96.65 ± 0.64 ^c	4.57 ± 0.21 ^{cd}	12.38 ± 0.47 ^{de}	97.55 ± 0.56 ^c
Xyl-AP	87.01 ± 1.28 ^e	8.55 ± 0.31 ^b	18.77 ± 0.19 ^b	89.42 ± 1.18 ^e
Mal-AP	97.76 ± 4.61 ^{bc}	4.79 ± 1.41 ^c	12.51 ± 2.16 ^{de}	98.71 ± 4.20 ^{bc}
MD-AP	104.26 ± 0.22 ^a	3.10 ± 0.04 ^e	11.19 ± 0.13 ^e	104.91 ± 0.22 ^a

L^* : brightness; a^* : stands for red and green; b^* : blue and yellow. Results are showed as mean values ± SD in triplicate. Values in the same columns showing the different letter are different significantly ($p < 0.05$)

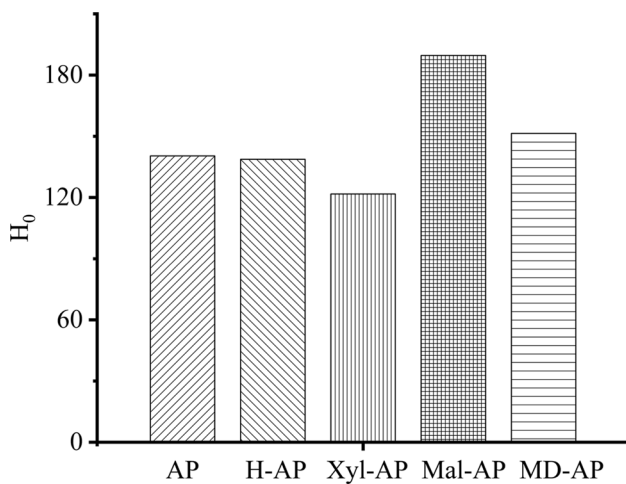


Fig. 14 Surface hydrophobicity of red bean protein mixture and glycosylation products. AP: red adzuki bean protein; H-AP: protein heated at 90 °C for 40 min; Xyl-AP, xylose glycosylated protein; Mal-AP, maltose glycosylated protein; MD-AP: maltodextrin glycosylated protein

to the exposure of chromophores by the protein unfolding during heat treatment. With the addition of saccharides, compared with H-AP, the peak intensity of the fluorescence emission peak of protein–saccharides mixture and its glycosylated conjugates became weaker, resulting in fluorescence quenching, which may be due to the shielding effect of the generation of saccharide chains on proteins.

Moreover, the maximum emission wavelength of the all the protein–saccharide conjugates all showed a red shift. The results of wavelength redshift and fluorescence intensity quenching indicated that tryptophan emitting group inside the protein was located in a more hydrophilic micro-environment and the interaction between saccharides and AP may occur [51]. This result also confirmed why the solubility of protein–saccharide conjugates was higher than that of the unmodified protein. Among the three kinds of protein–saccharide conjugates, the λ_{\max} of AP-Xyl had the maximum redshift and the fluorescence intensity was the weakest, which indicated that AP had the largest reaction activity with xylose, and the modification effect after glycosylation was the best, which was consistent with the emulsification activity and color properties.

Surface hydrophobic (H_0)

Surface hydrophobicity characterized the content of hydrophobic groups on the surface of proteins in polar environment, which was one of the most important indicators to evaluate protein denaturation [52].

Figure 14 showed the surface hydrophobicity of protein–saccharide conjugates. Compared to AP, H_0 was reduced in Xyl-AP but elevated in AP-Mal and AP-MD. In general, the surface hydrophobicity of the products reduced after glycosylation reaction. This could be attributed to two reasons: (1) the introduction of the hydrophilic hydroxyl group of the saccharide molecule. (2) the hydrophobic residues are blocked or the hydrophilic groups inside the protein are exposed [17]. It was known that maltose and maltodextrin were hydrophilic molecules, which would lead to the decrease of sample hydrophobicity. However, it may be that the reactivity of maltose and maltodextrin was not high enough to offset a large number of hydrophobic groups exposed outside the protein by heating, hence the protein molecules dominated the main role in their glycation products [53], leading to higher H_0 . The surface hydrophobicity of the three protein–saccharide conjugates corresponded to the results of their solubility.

Conclusions

In this study, alkali-soluble and acid-precipitation method was used to extract red adzuki bean protein. The optimal extraction process was determined as follows: the optimal extraction conditions were solid–liquid ratio 1:35 (w/v), pH 9.13, temperature 59 °C, and time 79.37 min. The functional characteristics of the AP showed that the solubility reached the optimum value (73.85%) at pH 10.0. At the AP concentration of 0.8%, the maximum emulsification (71.71 m²/g) and the minimum emulsification stability (11.8 min) were obtained. Three saccharides with different molecule sizes were used to prepare protein–saccharide conjugates. The functional properties of protein–saccharide conjugates were measured. The results indicated that all the protein–saccharide conjugates exhibited excellent FS when compared to AP and protein–saccharide mixtures. Upon analysis, it was found that Xyl-AP had the most effective emulsification function. The endogenous fluorescence spectroscopy and Fourier infrared spectroscopy (FTIR) results showed that the α -helix and β -folded structures decreased while the β -angle and random curling structures increased. The chromophore exposure caused fluorescence quenching, and the characteristic peaks changed correspondingly, which confirmed the occurrence of a glycosylation reaction.

The results of this study provide an effective method for the preparation and glycosylation of red adzuki bean protein. The results of the study on the structure and function of the protein and its glycosylated products will provide reference value for the development and utilization of red adzuki bean and its application in food and chemical

processing. Furthermore, protein–saccharide conjugates have demonstrated exceptional properties and will be further investigated.

Author contributions Chang Liu and Xiuli Wu: Conceptualization, methodology. Meng Li: Conceptualization, investigation, writing—original draft preparation. Juliang Huang and Yiming Chen: Software, validation, investigation, visualization.

Funding Scientific research project of Education Department of Jilin Province [JJKH20240752KJ], Scholar Climbing Program of Changchun University [zpk202122].

Data Availability Not applicable.

Declarations

Competing interests The authors state that there is no conflicts of interest.

References

- L.X. Wang, J. Wang, G.L. Luo, X.X. Yuan, D. Gong, L.L. Hu, S.H. Wang, H.L. Chen, X. Chen, X.Z. Cheng, Construction of a high-density adzuki bean genetic map and evaluation of its utility based on a QTL analysis of seed size. *J. Integr. Agric.* **20**(7), 1753–1761 (2021)
- S. Wu, S. Lu, J. Liu, S.Q. Yang, Q.J. Yan, Z.Q. Jiang, Physicochemical properties and bioactivities of rice beans fermented by *Bacillus amyloliquefaciens*. *Engineering* **7**(2), 219–225 (2020)
- R. Katoch, Nutritional potential of rice bean (*Vigna umbellata*): an underutilized legume. *J. Food Sci.* **78**(1), C8–C16 (2013)
- W.J. He, F.X. Guo, Y.T. Jiang, X.W. Liu, J. Chen, M.M. Zeng, Z.J. Wang, F. Qin, W.W. Li, Z.Y. He, Enzymatic hydrolysates of soy protein promote the physicochemical stability of mulberry anthocyanin extracts in food processing. *Food Chem.* **386**, 132811 (2022)
- P.C. Elena, J. Rocio, E.P. Julio, A. Manuel, V. Javier, Protein isolates from two Mediterranean legumes: *Lathyrus clymenum* and *Lathyrus annuus*. Chemical composition, functional properties and protein characterisation. *Food Chem.* **122**(3), 533–538 (2010)
- A.K. Stone, A. Karalash, R.T. Tyler, T.D. Warkentin, M.T. Nickerson, Functional attributes of pea protein isolates prepared using different extraction methods and cultivars. *Food Res. Int.* **76**, 31–38 (2015)
- M.X. Du, J.H. Xie, B. Gong, X. Xu, W. Tang, X. Li, C. Li, M.Y. Xie, Extraction, physicochemical characteristics and functional properties of Mung bean protein. *Food Hydrocolloids* **76**, 131–140 (2018)
- J.I. Boye, S. Aksay, S. Roufik, S. Ribéreau, M. Mondor, E. Farnworth, S.H. Rajamohamed, Comparison of the functional properties of pea, chickpea and lentil protein concentrates processed using ultrafiltration and isoelectric precipitation techniques. *Food Res. Int.* **43**(2), 537–546 (2010)
- L. Mirmoghtadaie, S.S. Aliabadi, S.M. Hosseini, Recent approaches in physical modification of protein functionality. *Food Chem.* **199**, 619–627 (2016)
- R. Pirestani, A. Nasirpour, J. Keramat, S. Desobry, Preparation of chemically modified canola protein isolate with gum Arabic by means of Maillard reaction under wet-heating conditions. *Carbohydr. Polym.* **155**, 201–207 (2017)
- J.X. Li, A.M. Shi, H.Z. Liu, H. Hu, Q. Wang, B. Adhikari, B. Jiao, M. Pignitter, Effect of hydrothermal cooking combined with high-pressure homogenization and enzymatic hydrolysis on the solubility and stability of peanut protein at low pH. *Foods*. **11**(9), 1289 (2022)
- X.X. Wang, Y.S. Li, Y. Zhou, F. Ma, P.J. Li, C.G. Chen, Effect of resistant corn starch on the thermal gelling properties of chicken breast myosin. *Food Hydrocolloids* **96**, 681–687 (2019)
- H.J. Lee, J.H. Kim, D.S. Ji, C.H. Lee, Effects of heating time and temperature on functional properties of proteins of yellow mealworm larvae (*Tenebrio molitor* L.). *Food Sci. Anim. Resour.* **39**(2), 296–308 (2019)
- C. Liu, Y.S. Xia, M. Hua, Z.M. Li, L. Zhang, S.S. Li, R.Z. Gong, S.X. Liu, Z.S. Wang, Y.S. Sun, Functional properties and antioxidant activity of gelatine and hydrolysate from deer antler base. *Food Sci. Nutr.* **8**(7), 3402–3412 (2020)
- Y.Y. Wang, A.Q. Zhang, Y.X. Wang, X.B. Wang, N. Xu, L.Z. Jiang, Effects of irradiation on the structure and properties of glycosylated soybean proteins. *Food Funct.* **11**(2), 1635–1646 (2020)
- W.D. Wang, C. Li, Z. Bin, Q. Huang, L.J. You, C. Chen, X. Fu, R.H. Liu, Physicochemical properties and bioactivity of whey protein isolate–inulin conjugates obtained by Maillard reaction. *Int. J. Biol. Macromol.* **150**, 326–335 (2020)
- B.L. Sun, P.X. Zhang, J.J. Zhang, Preparation, characterization and bioavailability studies of *Tegillarca granosa* hemoglobin and its glycosylated products. *Int. J. Biol. Macromol.* **219**, 11–20 (2022)
- M.A. Kurek, P.S. Anubhav, Plant-based (hemp, pea and rice) protein–maltodextrin combinations as wall material for spray-drying microencapsulation of hempseed (*Cannabis sativa*) oil. *Foods*. **9**(11), 1707 (2020)
- Q. Cui, L. Wang, G.R. Wang, A.Q. Zhang, X.B. Wang, L.Z. Jiang, Ultrasonication effects on physicochemical and emulsifying properties of *Cyperus esculentus* seed (tiger nut) proteins. *Cienc. Tecnol. Alim.* **142**, 110979 (2021)
- G. Yildiz, J.Z. Ding, J. Andrade, N.J. Engeseth, H. Feng, Effect of plant protein–polysaccharide complexes produced by manothermo-sonication and pH-shifting on the structure and stability of oil-in-water emulsions. *Innov. Food Sci. Emerg. Technol.* **47**, 317–325 (2018)
- D.C. Orsi, A.C.F. Nishi, V.S. Carvalho, E.R. Asquieri, Caracterização química, atividade Resistancee e formulação de doces com feijão azuki (*Vigna angularis*). *Braz. J. Food Technol.* **20**, e2016174 (2017)
- Y. Chen, L. Song, P. Chen, H.P. Liu, H.P. Liu, X.W. Zhang, Extraction, rheological, and physicochemical properties of water-soluble polysaccharides with antioxidant capacity from *Penthorum chinense* Pursh. *Foods*. **12**(12), 2335 (2023)
- X.F. He, B. Wang, B.T. Zhao, F. Yang, Ultrasonic assisted extraction of quinoa (*Chenopodium quinoa* Willd.) protein and effect of heat treatment on its in vitro digestion characteristics. *Foods* **11**(5), 771 (2022)
- M.Q. Tang, Q. Gao, Y. Xu, L. Zhong, X.W. Wang, J.W. Zhang, X. Peng, M. Tanokura, Y.L. Xue, Solubility and emulsifying activity of yam soluble protein. *J. Food Sci. Technol.* **57**, 1619–1627 (2019)
- M. Yuliana, C.T. Truong, L.H. Huynh, Q.P. Ho, Y.H. Ju, Isolation and characterization of protein isolated from defatted cashew nut shell: Influence of pH and NaCl on solubility and functional properties. *Cienc. Tecnol. Alim.* **55**(2), 621–626 (2013)
- K. Jahan, A. Ashfaq, R.U. Islam, K. Younis, O. Yousuf, Optimization of ultrasoundassisted protein extraction from defatted mustard meal and determination of its physical, structural, and functional properties. *J. Food Process. Preserv.* **46**(8), e16764 (2022)

27. S. Timr, D. Madern, F. Sterpone, Protein thermal stability. *Prog. Mol. Biol. Transl. Sci.* **170**, 239–272 (2020)
28. C. Magyar, M.M. Gromiha, Z. Savoly, I. Simon, The role of stabilization centers in protein thermal stability. *Biochem. Biophys. Res. Commun.* **471**(1), 57–62 (2016)
29. X. Zhao, J.L. Vazquez-Gutierrez, D.P. Johansson, R. Landberg, M. Langton, Yellow mealworm protein for food purposes—extraction and functional properties. *PLoS ONE* **11**(2), e0147791 (2016)
30. I.A. Wani, D.S. Sogi, U.S. Shivhare, B.S. Gill, Physico-chemical and functional properties of native and hydrolyzed kidney bean (*Phaseolus vulgaris* L.) protein isolates. *Food Rev. Int.* **76**, 11–18 (2015)
31. R. Niknam, M. Mousavi, H. Kiani, Comprehensive evaluation of emulsifying and foaming properties of *Gleditsia caspica* seed galactomannan as a new source of hydrocolloid: effect of extraction method. *Food Hydrocolloids* **131**, 107758 (2022)
32. C.T. Niu, Y.P. Han, J.J. Wang, F.Y. Zheng, C.F. Liu, Y.X. Li, Y.X. Li, Q. Li, Malt derived proteins: effect of protein Z on beer foam stability. *Food Biosci.* **25**, 21–27 (2018)
33. M. Tirgar, P. Silcock, A. Carne, E.J. Birch, Effect of extraction method on functional properties of flaxseed protein concentrates. *Food Chem.* **215**(15), 417–424 (2016)
34. Y. Tian, A. Taha, P.P. Zhang, Z. Zhang, H. Hu, S.Y. Pan, E.J. Birch, Effects of protein concentration, pH, and NaCl concentration on the physicochemical, interfacial, and emulsifying properties of β -conglycinin. *Food Hydrocolloids* **118**, 106784 (2021)
35. F. Liu, C.H. Tang, Soy glycinin as food-grade Pickering stabilizers: Part I. Structural characteristics, emulsifying properties and adsorption/arrangement at interface. *Food Hydrocolloids* **60**, 606–619 (2016)
36. S. Boostani, M. Aminlari, M. Moosavi-Nasab, M. Niakosari, G. Mesbahi, Fabrication and characterisation of soy protein isolate-grafted dextran biopolymer: a novel ingredient in spray-dried soy beverage formulation. *Int. J. Biol. Macromol.* **102**, 297–307 (2017)
37. J.F. Chen, Y. Yao, Phytoglycogen to enhance the solubility and in-vitro permeation of resveratrol. *Food Biophys.* **18**, 433–442 (2023)
38. M.B. Zia, S. Namli, M.H. Oztop, Physicochemical properties of wet-glycated soy proteins. *LWT Food Sci. Technol.* **142**, 110981 (2021)
39. T.D. Capar, H. Yalcin, Protein/polysaccharide conjugation via Maillard reactions in an aqueous media: Impact of protein type, reaction time and temperature. *LWT Food Sci. Technol.* **152**, 112252 (2021)
40. C.A. Manassero, M.C. Anon, F. Speroni, Development of a high protein beverage based on amaranth. *Plant Foods Hum. Nutr.* **75**, 599–607 (2020)
41. Y.F. Niu, Y. Li, Y.Q. Qiao, F. Li, D.F. Peng, W.Y. Shen, W.P. Jin, Q.R. Huang, In-situ grafting of dextran on oil body associated proteins at the oil–water interface through Maillard glycosylation: effect of dextran molecular weight. *Food Hydrocolloids* **146**, 109154 (2023)
42. W.J. Luo, H.Q. Lu, F.H. Lei, L.Y. Cheng, K. Li, W. Li, Structural elucidation of high-molecular-weight alkaline degradation products of hexoses. *Food Sci. Nutr.* **8**(6), 2848–2853 (2020)
43. J.J. Yu, G.Y. Chen, Y.F. Zhang, X.C. Zheng, P.Y. Jiang, H. Ji, S.H. Li, Y. Chen, Enhanced hydration properties and antioxidant activity of peanut protein by covalently binding with sesbania gum via cold plasma treatment. *Innov. Food Sci. Emerg. Technol.* **68**, 102632 (2021)
44. Q. Zhang, L. Li, Q.Y. Lan, M.L. Li, D.T. Wu, H. Chen, Y.W. Liu, D.R. Lin, W. Qin, Z.Q. Zhang, J. Liu, W.Y. Yang, Protein glycosylation: a promising way to modify the functional properties and extend the application in food system. *Crit. Rev. Food Sci. Nutr.* **59**(15), 2506–2533 (2018)
45. G.H. Bu, M.K. Ren, Y.X. Zuo, C.Y. Zhao, Functional characteristics and structural properties of soybean protein isolate–maltose conjugates. *Cereal Chem.* **99**(1), 100–110 (2021)
46. T.W. Zhu, L.Y. Ma, H.Y. Jiang, W.J. Li, X.F. Guo, C.X. Yang, G.H. Bu, Functional, structural properties of pea protein isolate-xylooligosaccharide glycosylated conjugate and its application in O/W emulsion preparation. *J. Food Meas. Charact.* **45** (2023)
47. G.Q. Huang, H.O. Wang, F.W. Wang, Y.L. Du, J.X. Xiao, Maillard reaction in protein–polysaccharide coacervated microcapsules and its effects on microcapsule properties. *Int. J. Biol. Macromol.* **155**(15), 1194–1201 (2019)
48. L.M. Jin, J. Bai, S.Y. Sui, Y.G. Hu, G.H. Niu, Optimization of microwave-assisted extraction of anthocyanins from adzuki bean seed coat by response surface methodology and its stability. *Sci. Technol. Food Ind.* **42**(6), 187–194 (2021)
49. C. Somjai, T. Siriwoharn, K. Kulprachakarn, S. Chaipoot, R. Phongphisutthinant, P. Wiriyacharee, Utilization of Maillard reaction in moist-dry-heating system to enhance physicochemical and antioxidative properties of dried whole longan fruit. *Heliyon* **7**(5), e07094 (2021)
50. S.Q. Xia, Y.Q. Li, Q.Y. Xia, X.M. Zhang, Q.R. Huang, Glycosylation of bovine serum albumin via Maillard reaction prevents epigallocatechin-3-gallate-induced protein aggregation. *Food Hydrocolloids* **43**, 228–235 (2015)
51. V.V. Khrustalev, V.V. Poboinev, A.N. Stojarov, T.A. Khrustaleva, Microenvironment of tryptophan residues in proteins of four structural classes: applications for fluorescence and circular dichroism spectroscopy. *Eur. Biophys. J.* **448**, 523–537 (2019)
52. S. Tang, J.S. Li, G.X. Huang, L.J. Yan, Predicting protein surface property with its surface hydrophobicity. *Protein Pept. Lett.* **28**(8), 938–944 (2021)
53. Y. Joubran, A. Moscovici, U. Lesmes, Antioxidant activity of bovine alpha lactalbumin Maillard products and evaluation of their in vitro gastro-duodenal digestive proteolysis. *Food Funct.* **6**(4), 1229–1240 (2015)

Publisher's Note Springer Nature remains neutral with regard to jurisdictional claims in published maps and institutional affiliations.

Springer Nature or its licensor (e.g. a society or other partner) holds exclusive rights to this article under a publishing agreement with the author(s) or other rightsholder(s); author self-archiving of the accepted manuscript version of this article is solely governed by the terms of such publishing agreement and applicable law.